ELSEVIER

Journal of Nuclear Materials 295 (2001) 205–212

journal of nuclear materials

www.elsevier.nl/locate/jnucmat

Consideration of the effects on fuel particle behavior from shrinkage cracks in the inner pyrocarbon layer

Gregory K. Miller *, David A. Petti, Dominic J. Varacalle, John T. Maki

Idaho National Engineering and Environmental Laboratory, P.O. Box 1625, Idaho Falls, ID 83415-3760, USA

Received 3 January 2001; accepted 5 March 2001

Abstract

The fundamental design for a gas-cooled pebble bed reactor relies on an understanding of the behavior of coated particle fuel. The coating layers surrounding the fuel kernels in these spherical particles consist of pyrolytic carbon layers and a silicon carbide (SiC) layer. These coating layers act as a pressure vessel that retains fission product gases. A small percentage of fuel particles may fail during irradiation in the mode of a traditional pressure vessel failure. Fuel performance models used to predict particle behavior have traditionally been one-dimensional models that focus on this failure mechanism. Results of irradiation experiments, however, show that many more fuel particles fail than would be predicted by this mechanism alone. Post-irradiation examinations indicate that multi-dimensional effects, such as the presence of shrinkage cracks in the inner pyrolytic carbon layer (IPyC), contribute to these unexplained failures. Results of a study performed to evaluate the significance of cracking in the IPyC layer on behavior of a fuel particle are presented herein, which indicate that shrinkage cracks could contribute significantly to fuel particle failures.

1. Introduction

The success of gas-cooled reactors depends largely upon the safety and quality of the coated particle fuel. The coating layers in the particles, which surround uranium oxycarbide fuel kernels, consist of pyrolytic carbon layers and a silicon carbide layer. Typically the kernel is coated with a porous pyrolytic carbon layer called the buffer. Next an inner pyrolytic carbon layer (IPyC) is placed on the buffer, which is followed by a layer of silicon carbide (SIC). An outer pyrolytic carbon layer (OPyC) is then placed on top of the SiC. The outer three layers (IPyC, SiC, OPyC) act as a pressure vessel for fission product gases as well as a barrier to the migration of other fission products. The quality of the fuel relies on minimizing the number of failures of these particles during reactor operation. Therefore, a performance model of the coating layers is needed to determine the failure probabilities of a population of fuel particles. Such a model must account for all viable mechanisms that can lead to particle failure.

Historically, symmetric one-dimensional models have been developed for examining and predicting fuel particle behavior. For example, prior investigations at the Idaho National Engineering and Environmental Laboratory (INEEL) have been conducted using the FUEL code [1]. This is a stand-alone code that uses the Monte Carlo technique to calculate the expected failure probability in a statistical sample of TRISO-coated fuel particles during normal operation of the new production-modular high-temperature gas-cooled teactor (NP-MHTGR). The mode of failure considered in the code is a pressure vessel failure caused by the buildup of fission gas pressure in the kernel of the particle. The code was designed to be efficient at sampling large populations of particles to investigate the low failure rates anticipated for the NP-MHTGR. The code considers statistical variations in a number of input parameters including kernel diameter, buffer thickness, thicknesses of the pyrocarbon and silicon carbide layers, kernel and buffer densities, and strength of the silicon carbide layer. While the code itself solves for a perfectly spherical particle, it

* Corresponding author.
E-mail address: gkm@inel.gov (G.K. Miller).

0022-3115/01/$ - see front matter
PII: S0022-3115(01)00551-7

Nomenclature

E	Young's modulus for SiC layer (MPa)
m	Weibull modulus for IPyC layer
P_f	Probability of failure for the IPyC layer
V	Volume of the IPyC or SiC layer (μm^3)
v	Poisson's ratio for the SiC layer
σ	Stress in the IPyC layer (MPa)
σ_0	Weibull characteristic strength for the IPyC layer (MPa $\mu m^{3/m}$)
σ_{max}	Maximum principal tensile stress anywhere in the IPyC layer (MPa)
σ_{mc}	Weibull mean strength for the IPyC layer (MPa)
σ_i	$i = 1, 2, 3$, Principal stress components in three orthogonal directions (MPa)

has been shown that it can be used in conjunction with finite element analyses to produce a failure probability for a batch of a aspherical particles [2].

The fuel of the NP-MHTGR as well as other coated fuel designed in the US have incurred significantly greater failure percentages than are predicted considering just the pressure vessel failures of a one-dimensional code, indicating that other mechanisms contribute to failure of the particles. Post-irradiation examination (PIE) revealed the presence of radial shrinkage cracks in the IPyC and OPyC layers, and partial debonding between the IPyC and the SiC. It is postulated that these multi-dimensional effects may have led to the unexpectedly large number of failures of fuel particles in the US. The focus of the investigation performed herein is to evaluate the significance of cracking in the IPyC layer on behavior of a particle. Evaluations of other mechanisms, such as debonding of the IPyC, are reserved for separate investigation.

2. Consideration of shrinkage crack in inner pyrocarbon layer

As stated above, it is postulated that shrinkage cracks in the IPyC layer contributed significantly to the failures experienced in US fuel particles. This depends first on how prevalent these cracks are in a typical batch of fuel particles. Because the IPyC layer incurs significant circumferential tensile stresses during irradiation of the particle, it is surmised that cracks in the IPyC layer are caused by the shrinkage of the IPyC layer that occurs during this time. Evaluating the potential for cracking in the IPyC layer required that stress analyses be performed to determine the stress state in the uncracked particle. Once the potential for cracking was demonstrated, then stress analyses were performed on cracked particles to assess the effects that these cracks have on particle behavior.

A typical TRISO-coated particle is shown in Fig. 1. Fission gas pressure builds up in the kernel and buffer regions, while the IPyC, SiC, and OPyC act as structural layers to retain this pressure. The ABAQUS program

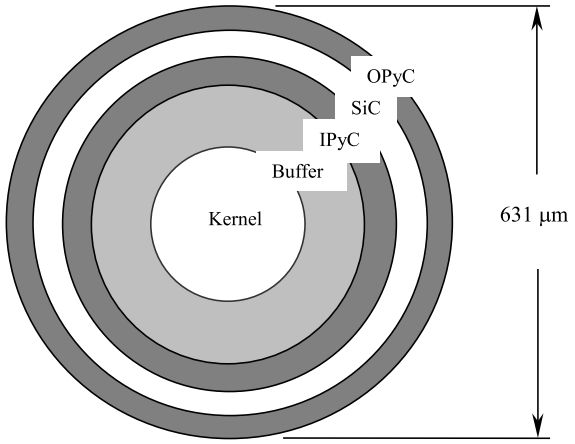

Fig. 1. Typical TRISO-coated fuel particle geometry.

has been used previously to analyze the TRISO-coated particles of the NP-MHTGR [3,4]. The basic behavior modeled in these analyses (as well as the FUEL Code) is shown schematically in Fig. 2. The IPyC and OPyC layers both shrink and creep during irradiation of the particle while the SiC exhibits only elastic response. A portion of the gas pressure is transmitted through the IPyC layer to the SiC. This pressure continually

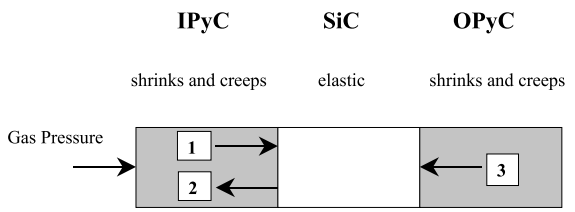

1 Gas pressure is transmitted through the IPyC

2 IPyC shrinks, pulling away from the SiC

3 OPyC shrinks, pushing in on SiC

Fig. 2. Behavior of coating layers in fuel particle.

increases as irradiation of the particle progresses, thereby contributing to a tensile hoop stress in the SiC layer. Countering the effect of the pressure load is the shrinkage of the IPyC during irradiation, which pulls inward on the SiC. Likewise, shrinkage of the OPyC causes it to push inward on the SiC. Failure of the particle is normally expected to occur if the stress in the SiC layer reaches the fracture strength of the SiC. Failure of the SiC results in an instantaneous release of elastic energy that should be sufficient to cause simultaneous failure of the pyrocarbon layers.

The methodology presented in [3] is employed here to perform finite element analysis on fuel particles. The model used in [3], however, assumed full spherical symmetry, thereby requiring only a single layer of particles. The models used here are axisymmetric models that allow for non-symmetry in the plane, thus enabling an evaluation of multi-dimensional effects.

2.1. Analysis of normal particle

The first analysis performed is that of a normal spherical particle having no cracks or defects in the layers of the particle. The IPyC and OPyC layers are assumed to remain fully bonded to the SiC layer throughout irradiation. This analysis is intended to demonstrate behavior of a normal particle in expected reactor conditions, as well as to determine stresses in the IPyC layer throughout the irradiation. The model used for this case, which consists of 4-node quadrilateral elements (designated CAX4I in ABAQUS), is shown in Fig. 3. Only the three structural layers (i.e., the IPyC, SiC, and OPyC) of the particle are included in the model. The elements used are axisymmetric, giving the model the effect of a full sphere. The layer thicknesses and overall dimensions are typical of a fuel particle in a pebble bed reactor. Specifically, the layer thicknesses for the IPyC, SiC, and OPyC are 40, 35, and 43 μm, respectively. The kernel diameter and buffer thickness are 195 and 100 μm, respectively, resulting in an outside particle diameter of 631 μm. The internal pressure applied in this analysis was ramped linearly from zero at the beginning of irradiation to a final value of 23.7 MPa, which is typical of conditions expected for a gas-cooled reactor. Also applied was a constant external pressure of 6.4 MPa to represent ambient reactor conditions.

Numerous material properties were needed to represent fuel particle behavior in the ABAQUS model. These included irradiation-induced strain rates used to represent shrinkage (or swelling) of the pyrocarbon layers, creep coefficients to represent irradiation-induced creep in the pyrocarbon layers, and elastic properties to represent elastic behavior for the pyrocarbons and silicon carbide. The properties used in the analysis were obtained from data that were compiled in a report by the CEGA Corporation in July 1993. These data were based on a review and evaluation of material properties published in the literature to that date (Refs. [5–11]).

Due to anisotropy in the swelling behavior of the pyrocarbon layers, the strains are different for the radial and tangential directions. The swelling strains are reported in the CEGA data to be functions of four variables, i.e., fluence level, pyrocarbon density, degree of anisotropy (as measured by the Bacon anisotropy factor, BAF), and irradiation temperature. Fig. 4 shows swelling strains as a function of fluence and BAF for the radial and tangential directions. The plots presented correspond to a pyrocarbon density of 1.96×10^6 g/m^3 and an irradiation temperature of 1032°C, and cover a range of BAF from 1.02 to 1.28. In the radial direction, the pyrocarbon shrinks at low fluences but swells at higher fluences for all but the lowest BAF values. In the tangential direction, the pyrocarbon continually shrinks at all levels of fluence and the magnitude of the

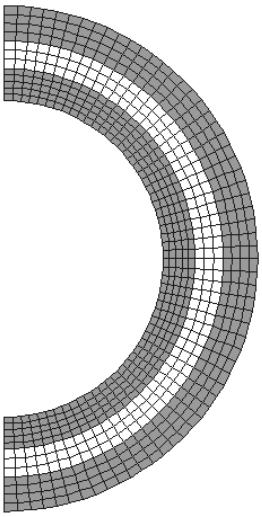

Fig. 3. Finite element model for TRISO-coated fuel particle showing IPyC, SiC, and OPyC layers.

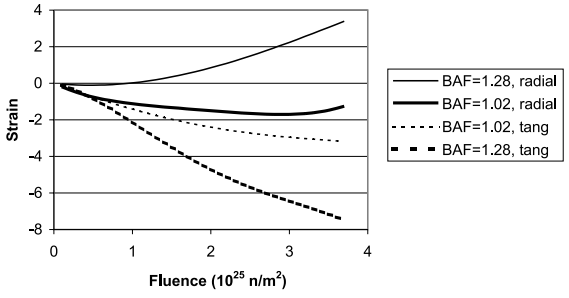

Fig. 4. Radial and tangential swelling (shrinkage) of pyrocarbon for variations in BAF.

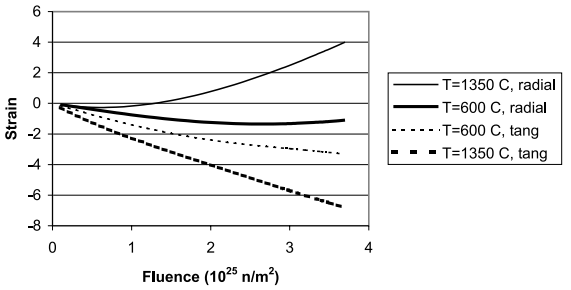

Fig. 5. Radial and tangential swelling (shrinkage) of pyrocarbon for variations in temperature.

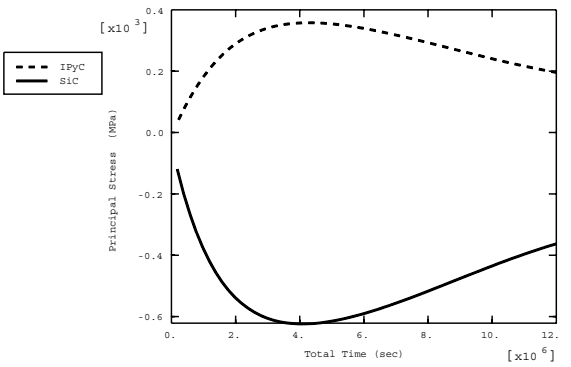

Fig. 6. Stress histories at inner radii of the IPyC and SiC layers for an uncracked particle.

shrinkage increases as the BAF increases. Fig. 5 shows swelling strains as a function of fluence and temperature for the radial and tangential directions. The plots presented correspond to a pyrocarbon density of 1.96×10^6 g/m^3 and a BAF value of 1.08, and cover a range of temperature from 600°C to 1350°C. Similar trends are seen in these curves, wherein the magnitude of shrinkage increases as the temperature increases.

In the ABAQUS model, the swelling data were input in the form of strain rates that are functions of four field variables, i.e., fluence level, pyrocarbon density, BAF, and irradiation temperature. Irradiation-induced creep in the pyrocarbon layers was treated as secondary creep, i.e., the creep strain rate was proportional to the level of stress in the pyrocarbon. The creep coefficient was applied as a function of pyrocarbon density and irradiation temperature. The Young's modulus for the pyrocarbon layers was applied as a function of four variables (the same variables as used for swelling), while the Young's modulus for the silicon carbide layer was applied only as a function of temperature. Values of 0.33 and 0.13 were used for Poisson's ratio in the pyrocarbon and SiC layers, respectively.

The particle was analyzed for the pressure, creep, and swelling that act during the irradiation of the particle. This was done in a viscoelastic time-integration analysis that progressed until the fluence reached 3×10^{25} n/m^2, occurring at a time of 1.2×10^7 s in the analysis. For the particle analyzed, a density of 1.9×10^6 g/m^3 and a BAF of 1.16 were assumed for both the IPyC and OPyC layers. The irradiation temperature was assumed to be a constant 1200°C.

Fig. 6 plots a time history for the tangential stress that was calculated for the inner surface of the SiC. This shows that early during irradiation, the shrinkage of the pyrocarbon layers induces a steadily increasing compressive stress in the SiC. Eventually, though, creep in the pyrocarbon layers relieves stress in those layers, diminishing the beneficial effect of the shrinkage. Additionally, the internal pressure continually increases as irradiation progresses. Therefore, the tangential stress in the SiC reaches a minimum value and then steadily increases through the remainder of irradiation. Failure of such a particle would occur if the stress eventually becomes tensile and reaches the fracture strength of the SiC material. This would be a classic pressure vessel failure, occurring well into irradiation of the particle. Calculations have shown that failure in this mode is predicted to occur in only a very small percentage of particles.

Fig. 6 also plots a time history for the tangential stress at the inner surface of the IPyC. Early during irradiation, shrinkage of the IPyC induces a steadily increasing tensile stress in that layer. Eventually, creep in the IPyC begins to relieve the tensile stress in this layer. Therefore, the tangential stress in the IPyC reaches a maximum value and then steadily decreases through the remainder of irradiation.

2.2. Stresses in the IPyC layer

Because the shrinkage and creep behavior of the pyrocarbons were modeled as functions of four variables, including anisotropy, it was possible to evaluate the sensitivity of stresses in the IPyC to the degree of anisotropy (as measured by the BAF). Therefore,

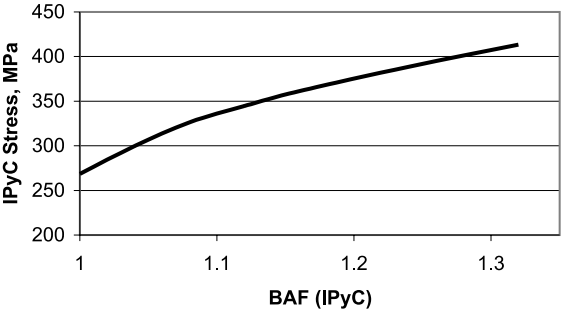

Fig. 7. Maximum stress in IPyC layer as a function of BAF.

ABAQUS calculations were performed for BAFs ranging from 1.0 to 1.33. Results are shown in Fig. 7, where the maximum IPyC stress calculated at any time during irradiation is plotted against the BAF value. Results show that the IPyC stress is quite sensitive to the BAF, increasing by about 50% as the BAF is changed from 1.0 to 1.33.

Because of the brittle nature of pyrolytic carbon, the IPyC is expected to fail in a probabilistic manner according to the Weibull statistical theory [12]. As such, the failure probability for the IPyC in a batch of particles is given by

$$P_f = 1 - e^{-\int_V (\sigma/\sigma_0)^m \, dV} \quad (1)$$

or

$$P_f = 1 - e^{-(\sigma_{max}/\sigma_{mc})^m}. \quad (2)$$

Based on CEGA's data for the pyrocarbons, the Weibull modulus m is expected to be about 9.5, while the mean strength σ_{mc} is about 300 MPa. The data indicate that the strength actually increases with BAF, but it is not clear that this trend continues for BAF > 1.1. Therefore, a strength dependence on BAF is neglected in this calculation. Fig. 8 presents the calculated failure probability for the IPyC as a function of BAF, which shows that the increase in stress due to BAF results in an increase in failure probability from 30% at a BAF of 1.0 to 100% at a BAF of 1.33. These results show not only that the failure probability in the IPyC is sensitive to BAF, but also that a significant number of failures in the IPyC (~30%) can occur even at very low levels of anisotropy. This means that shrinkage cracks in the IPyC are likely to be prevalent among fuel particles having an IPyC that is bonded to the SiC, and therefore should be evaluated for their effects on the behavior of fuel particles.

It must be clarified that the probability calculated pertains only to particles having an IPyC that remains bonded to the SiC. If the IPyC fully debonds from the SiC, then stresses are not transmitted between the two layers, and cracking of the IPyC is irrelevant.

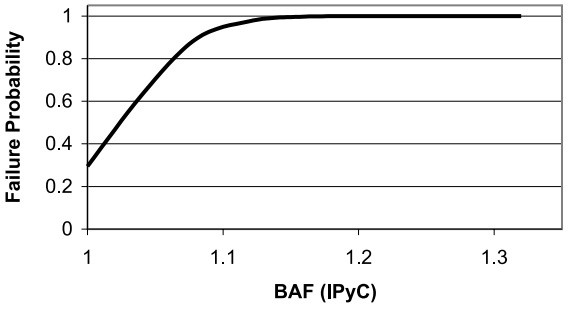

Fig. 8. Failure probability of IPyC layer as a function of BAF.

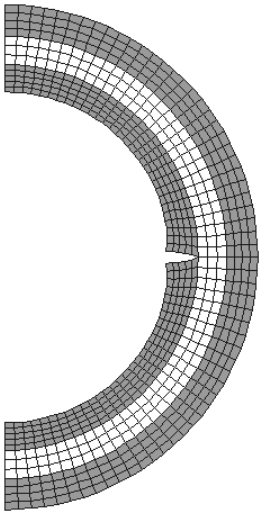

Fig. 9. Finite element model for fuel particle having radial crack in IPyC layer.

2.3. Analysis of cracked particle

Analyses were performed on a spherical particle having a radial crack through the thickness of the IPyC layer. The model used for these analyses (Fig. 9) is identical in all other respects to that described for the normal particle above. The crack is typical of those observed in PIEs of the NP-MHTGR fuel particles, as shown in Fig. 10. The particle shown in this photograph has a fourth coating layer known as a protective pyrocarbon. It is surmised that the crack in the IPyC is formed sometime after initial irradiation of the particle, and is caused by irradiation-induced shrinkage of the

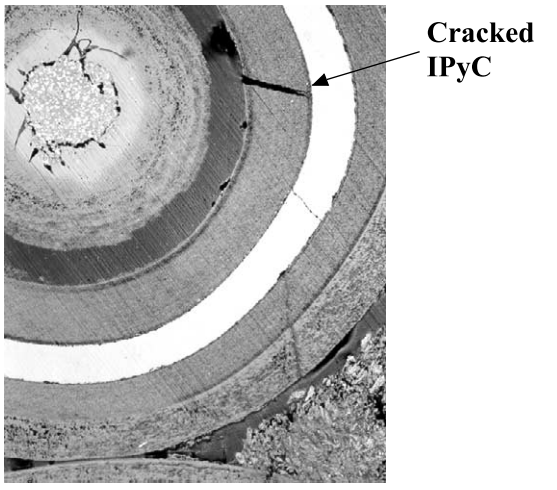

Fig. 10. Radial cracks in IPyC observed from post-irradiation examination.

IPyC layer. It is included in the model from the beginning of the solution since it is not feasible to initiate the crack later in the analysis. Because the shrinkage in the pyrocarbons dominates the particle behavior early during irradiation, large tensile stresses in the IPyC occur early. Therefore, the assumption of the presence of a crack at the beginning of the solution should be a reasonable approximation. The analysis does not include any dynamic effects associated with a sudden failure of the IPyC, which could increase the magnitude of the stresses calculated.

Because the model is axisymmetric, the crack in the IPyC effectively extends around the full circumference of the particle. The stress analysis for this cracked configuration shows a stress concentration in the SiC layer in the vicinity of the crack tip. Fig. 11 plots a time history for the maximum principal stress in the SiC layer as calculated in ABAQUS at an integration point near the crack tip. Because the calculated stresses become discontinuous at the crack tip, it is not feasible to accurately calculate stresses right at the tip. Contrary to the stress history of Fig. 6 for a normal particle, the maximum stress around the crack tip quickly becomes tensile, rising to a peak value of 398 MPa early in irradiation (at a fluence of about 1×10^{25} n/m^2). Creep in the pyrocarbon layers eventually starts to relieve stress in those layers, and the stress around the crack tip correspondingly falls off. The stresses around the crack tip reach a peak well before the internal pressure has reached a full value.

The case of the cracked IPyC was run with a wide variation in the internal pressure loading. It was found in these analyses that the peak tensile stress was insensitive to the magnitude of the internal pressure applied. This suggests that failure of a particle that has developed a crack in the IPyC layer is no longer governed by internal pressure loading. This result pertains to the kernel diameter assumed for these analyses of 195 μm. For particles having larger kernel diameters, analyses show

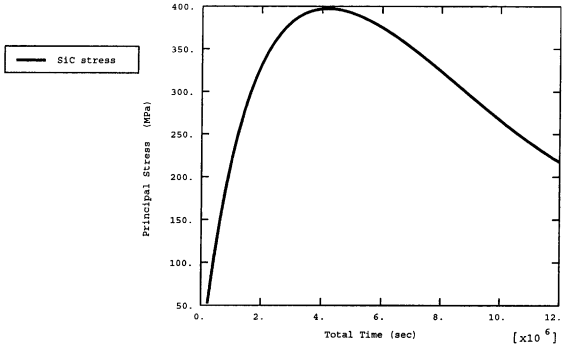

Fig. 11. Stress history in SiC layer (near crack tip) for cracked particle.

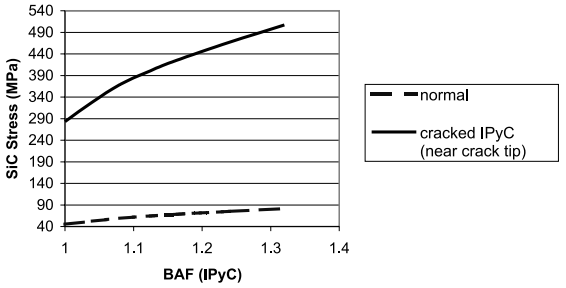

Fig. 12. Stress in SiC layer as a function of BAF for normal and cracked particles.

that stresses around the crack tip can be significantly affected by internal pressure as irradiation progresses.

Several analyses were run to determine the effect of variations in BAF of the IPyC on the stress in the SiC layer. In these calculations, the BAF of the OPyC was set equal to 1.04. Results are presented in Fig. 12, where it is shown that the SiC stress increases as the BAF (of the IPyC) increases. It is evident that the SiC stress is sensitive to the BAF for both the cracked and the normal (uncracked) particles. The results suggest that the BAF is an important parameter relative to stresses in the SiC layer, which could consequently affect the number of particle failures.

3. Failure evaluation of a particle having a cracked IPyC

The question arises as to whether the stresses around the crack tip are large enough to fail the particle. A fracture mechanics evaluation to determine whether a cracked IPyC layer results in failure of the SiC would require the calculation of a stress intensity at the crack tip. Such a calculation is greatly complicated by the fact that there is a material discontinuity at the interface between the IPyC and SiC layers. Therefore, the Weibull definition of failure probability was applied to evaluate the potential for failure of the SiC. Once finite element results were obtained from the analysis of the cracked particle, the stress integration of Eq. (1) was performed using the principle of independent action (PIA) model for treating multiaxial stress states [12]:

$$\int_V \sigma^m \, \mathrm{d}V = \int_V \left(\sigma_1^m + \sigma_2^m + \sigma_3^m\right) \mathrm{d}V. \tag{3}$$

Since only tensile stresses contribute to fracture of the material, compressive stresses were not included in this integration. Only stresses in four finite elements of the SiC layer in the immediate vicinity of the crack tip made a meaningful contribution to this integral. The integral was dominated by component σ_3, the maximum

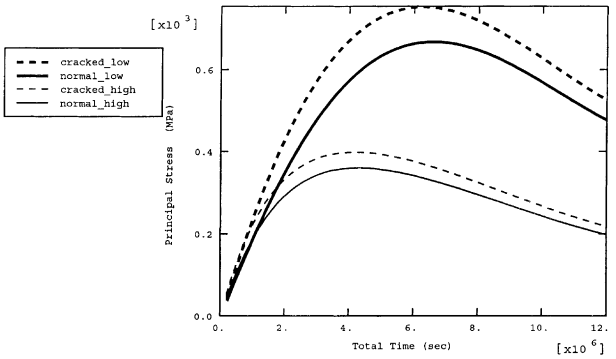

Fig. 13. Stress histories for normal and cracked particles, low temperature vs. high temperature.

of the three principal stresses; the minimum stress σ_1 was always negative, and therefore made no contribution.

A characteristic strength σ_0 of 9640 MPa $\mu m^{3/6}$ and a modulus m of 6 were assumed for the SiC layer, in accordance with the material property data compiled by CEGA. Substitution into Eq. (1) then gave a failure probability for the SiC layer of 0.001. This probability is high enough to indicate that cracking of the IPyC layer could be a significant contributor to the failure of fuel particles and should be included in performance models used to predict fuel behavior. The calculated probability does not account for statistical variations in layer thicknesses, pyrocarbon density, and the pyrocarbon BAF that may occur among particles in a batch, which could increase the failure probability.

4. Effects of low temperature

The calculations discussed so far all corresponded to an irradiation temperature of 1200°C. The material properties input to the ABAQUS model allow temperature variations from 600° to 1350°C. Temperature variations affect the elastic, swelling, and creep properties of the pyrocarbon layers as well as the elastic properties of the silicon carbide layer. Thus, analyses were performed at a temperature of 600°C to determine the effects that this low irradiation temperature has on stresses in both a normal particle and a particle having a crack in the IPyC layer.

A time history for the tangential stress at the inner surface of the IPyC layer in a normal particle is presented as the curve 'normal_low' in Fig. 13. Comparing this to the stress for a particle at 1200°C 'normal_high', it is evident that the lower temperature causes a substantial increase in the IPyC stress. Because swelling in the IPyC layer is significantly less at the lower temperature, it might be expected that the tensile stress in the IPyC would decrease. However, the creep coefficient in the pyrocarbons at 600°C is only about 1/3 of the coefficient at 1200°C. This lower creep fails to relax the stress in the IPyC until the stress well exceeds that attained at the higher temperature.

A similar effect occurs for stresses in the SiC layer of a particle having a crack in the IPyC layer. Fig. 13 presents a time history for the maximum calculated principal stress in the SiC layer near the crack tip for an irradiation temperature of 600°C 'cracked_low'. Comparing this to the stress for a particle at 1200°C 'cracked_high', it is evident that the lower temperature causes a substantial increase in the SiC stress. Again, the lower creep of the pyrocarbons fails to relax stresses in the SiC layer until the stress well exceeds that attained at the higher temperature.

5. Conclusions

Based on the evaluations performed herein concerning the effects of shrinkage cracks in the IPyC layer on fuel particle behavior, the following conclusions are made.

- The mode of failure normally assumed for a TRISO-coated particle is a classic pressure vessel failure. Predictions indicate that this failure mechanism alone does not explain the failure percentages that have occurred in fuel particle irradiations.
- The probability for cracking in the IPyC is significant for particles where the IPyC remains bonded to the SiC layer. This indicates that cracks in the IPyC need to be considered for their effects on fuel particle behavior.
- Treating the material properties for the pyrocarbon layers as a function of anisotropy (BAF) has enabled a determination of the sensitivity of particle stresses to variations in BAF. Calculations show that the tangential tensile stress in the IPyC layer is very sensitive to the BAF. Consequently, the probability for cracking in the IPyC layer is sensitive to the BAF, making this an important consideration in fuel particle

design. It was also shown that stresses in the SiC layer are sensitive to the BAF, whether or not the IPyC is cracked, which can directly affect the number of particle failures.

- For the size of particle analyzed, stresses around the crack tip of a particle having a cracked IPyC are insensitive to the magnitude of internal pressure applied. This suggests that failure of such a particle is not governed by internal pressure loading. For particles having larger kernel diameters (>200 μm), though, analyses show that stresses around the crack tip can be significantly affected by internal pressure as irradiation progresses.
- A failure evaluation showed that cracks in the IPyC layer could contribute significantly to the failure probability for a batch of fuel particles. Therefore, this failure mechanism should be included in performance models that predict fuel particle behavior.
- Calculations indicate that a decrease in irradiation temperature from 1200°C to 600°C significantly increases the tensile stress in the IPyC layer of a normal particle and the stresses in the vicinity of the crack tip of a particle having a cracked IPyC. Shrinkage of the IPyC layer is diminished at the lower temperature, but this is more than offset by a reduction in stress relaxation caused by a substantially smaller creep coefficient.
- Future study is needed to investigate the effects of variations in fuel particle design parameters from the nominal condition, which include variations in particle geometry and material properties. Variations in these parameters will be examined for their effect on stress levels and failure probabilities. Detailed studies will also be performed on the effects of debonding between particle layers.

Acknowledgements

This work was supported through the INEEL Long-Term Research Initiative Program under DOE Idaho Operations Office Contract DE-AC07-99ID13727.

References

[1] R.G. Bennett, G.K. Miller, L.H. Menke, User's Manual for the NP-MHTGR Fuel Code, EG&G Idaho, Inc., Idaho National Engineering and Environmental Laboratory, 1993.
[2] G.K. Miller, D.C. Wadsworth, J. Nucl. Mater. 211 (1994) 57.
[3] R.G. Bennett, Nucl. Technol. 96 (1991) 117.
[4] G.K. Miller, R.G. Bennett, Finite element stress analysis of NP-MHTGR target particles with the ABAQUS code, Idaho National Engineering and Environmental Laboratory, 1991.
[5] J.L. Kaae, J. Nucl. Mater. 46 (1973) 121.
[6] J.L. Kaae, J.C. Bokros, D.W. Stevens, Carbon 10 (1972) 571.
[7] J.C. Bokros, R.W. Dunlap, A.S. Schwartz, Carbon 7 (1969) 143.
[8] J.C. Bokros, G.L. Guthrie, R.W. Dunlap, A.S. Schwartz, J. Nucl. Mater. 31 (1969) 25.
[9] J.L. Kaae, J.C. Bokros, Carbon 9 (1969) 111.
[10] J.L. Kaae, D.W. Stephens, J.C. Bokros, Carbon 10 (1972) 561.
[11] J.L. Kaae, Carbon 12 (1974) 577.
[12] N.N. Nemeth, J.M. Mandershield, J.P. Gyekenyesi, Ceramics Analysis and Reliability Evaluation of Structures (CARES) User's and Programmer's Manual, NASA Technical Paper 2916, 1989.